Relationship between the charge-coupled device signal-to-noise ratio and dynamic range with respect to the analog gain

Dejiang Wang,[1,2,3,*] Tao Zhang,[2] and Haipeng Kuang[1,2]

[1]Key Laboratory of Airborne Optical Imaging and Measurement, Changchun Institute of Optics,
Fine Mechanics and Physics, Chinese Academy of Sciences, Changchun 130033, China

[2]Changchun Institute of Optics, Fine Mechanics and Physics, Chinese Academy of Science, Changchun 130033, China

[3]Graduate School of the Chinese Academy of Science, Beijing 100084, China

*Corresponding author: wangdj04@ciomp.ac.cn

The signal-to-noise ratio and the dynamic range are the two key parameters characterizing CCD performance, especially in remote sensing applications. After exploring the possible sources of CCD noise, this paper analyzes the impacts of the analog gain on the two parameters, respectively, and establishes the mathematical models describing their relationships. Then the platforms including the CCD radiometric calibration and imaging in practice are constructed to test the proposed models based on two situations, considering the influence of the quantization noise. Finally, the design trade-off between the signal-to-noise ratio and the dynamic range is presented, such that the CCD signal-to-noise ratio will be improved as much as possible, while the dynamic range degradation becomes acceptable.   © 2012 Optical Society of America

OCIS codes: 040.1520, 110.4280, 010.0280, 100.2980.

1. Introduction

Since CCD has the virtues of low noise, high dynamic range, high quantum efficiency, and wide spectral response, it has been widely used in general imaging, machine vision, and scientific and military applications [1–3]. Recently, China launched its second unmanned lunar probe, Chang'eII. The key payload of the spacecraft was a CCD stereo camera. As reported, its ground resolution could reach 1 m in the 100 km × 15 km elliptical orbit. It is well known that the higher the CCD signal-to-noise ratio (SNR) is, the more useful information could be extracted from the lunar surface images. Nevertheless, limited by the storage capability and transmission bandwidth in the spacecraft, the captured images are

usually rounded to 8 bits, which leads to the CCD SNR losses as well as the system dynamic range degradation [4], especially under low illuminations. Taking larger aperture and longer integration time are the two common methods to improve the CCD SNR in remote imaging systems. Unfortunately, the primary mirror diameter for the space camera is limited by the volume and mass constraints of the launch vehicles as well as the scaling laws of manufacturing costs [5], while the longer exposure time will result in excessive motion between photosensitive pixels and the objects, which leads to the image quality degradation greatly [6,7]. In addition, digital and analog gain adjustments that are implemented in many modern CCD cameras could also enhance the video signal intensities for improving the image interpretability, and it seems that they could improve the CCD SNR. However, digital gain adjustment is a pure mathematical operation to the

captured images; the signals including the valid video and the corresponding noises are increased by the same factor, so it is irrelevant to the CCD SNR [8]. While analog gain adjustment is a processing component embedded in the CCD cameras, the image sensors could exhibit their optimum capacity by appropriate gain factor settings [9]. Nevertheless, the factory analog gain values are mainly applicable to the condition where the illumination is relatively high and the influence of quantization noise could be neglected. Meanwhile for remote sensing applications where the illumination is relatively low, the impacts of the analog gain to the CCD SNR as well as the dynamic range, to our knowledge, are lacking from the literature. Therefore there is an urgent requirement on how to determine the most suitable gain factor, such that the CCD performance could be optimized as well as possible.

There are two main objectives in this paper. First, we will try to explore the mathematical models describing the relationship between the CCD SNR and the dynamic range with respect to the analog gain, and second, we will test the proposed models through experiments, where four issues relating to the analog gain adjustment will be investigated: (1) the CCD individual noise sources, (2) the CCD SNR augmenter, (3) the CCD dynamic range, and (4) the real image quality. And then we will find the appropriate gain factors for practical applications.

2. CCD Noise Models

An overview of the CCD noise sources is available in [1,2]. Based on that model, we illustrate the CCD signal transfer diagram in Fig. 1. Once exposure of all pixels is finished, the sensor transfers its aggregate charges to the readout registers, which feed each pixel's charges from the image sensor into an output node that converts the charges into voltages. After the charges transfer and conversion, the voltages are amplified to become the camera's analog outputs. Finally, the analog-to-digital (A/D) converter converts voltages to digital numbers. Each noise source is given in Fig. 1, and the complete noise model and
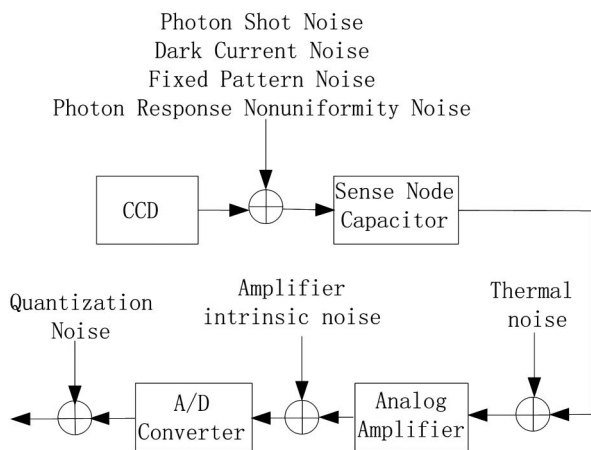

Fig. 1. Noise model of the CCD.

their noise equivalent power are shown in Table 1 [10,11]. Given a fixed CCD sampling frequency, all sources are considered additive Gaussian distribute. Considering the detector in the presence of signal as well as background radiation, the equation for the power of the total noisy N^2 is

$$N^2 = g^2 \langle N^2_{\text{shot}}(P_S + P_B) \rangle + g^2 \langle N^2_{\text{PRNU}}(P_S + P_B) \rangle$$
$$+ g^2 \langle N^2_T \rangle + g^2 \langle N^2_{\text{Dark}} \rangle + g^2 \langle N^2_{\text{FPN}} \rangle + \langle N^2_I \rangle + \langle N^2_Q \rangle,$$
$$(1)$$

where g represents the analog gain factor.

The dark current noise, the fixed pattern noise, and the thermal noise are the intrinsic components of the image sensors, which are illumination independent. Generally, they are referred to as the floor noise of the CCD:

$$\langle N^2_{\text{floor}} \rangle = \langle N^2_{\text{Dark}} \rangle + \langle N^2_{\text{FPN}} \rangle + \langle N^2_T \rangle. \quad (2)$$

The photo response nonuniformity (PRNU) noise is the variation in pixel responsivity. It is traditionally expressed as a fraction of the total number of the charge carriers. This approach assumes that the detectors are operating in a linear region with the responsivity difference only. If A is the fixed pattern ratio, then

$$\langle N^2_{\text{PRNU}}(P_S + P_B) \rangle = AI^2, \quad (3)$$

where I is the summation of the valid signal power and the background power.

The photon shot noise arises from the random fluctuations in the arrival rate of photons, and it follows a Poisson distribution. Therefore, the variance of the photon shot noise equals the expected signal level, so that

$$\langle N^2_{\text{shot}}(P_S + P_B) \rangle = BI, \quad (4)$$

where B represents the ratio of the sampled signal to the photon shot noise.

The floor noise is a function of the integration time and the operating temperature, which are almost invariable during the course of imaging, so it is represented by the constant, C.

The amplifier intrinsic noise and the quantization noise come after the analog amplifier; thus they are analog gain independent. Then they are represented by the variable, D.

Despite the various noise sources that exist, it is sufficient enough to consider the photon shot noise, the PRNU noise, the floor noise, the amplifier intrinsic noise, and the quantization noise for many applications. So, the total noise is represented as a combination of the aforementioned five types of noise sources. Substituting Eqs. (2)–(4) into Eq. (1), replacing the floor noise with C, and replacing the combinations of the amplifier intrinsic noise and the A/D converter quantization noise with D, the power of the CCD total noise is expressed as

$$\langle N^2 \rangle = Ag^2 I^2 + Bg^2 I + g^2 C + D. \quad (5)$$

3. SNR and Dynamic Range Models with the Analog Gain

A. Mathematical Models of the CCD SNR with the Analog Gain

The magnitude of the video signal leaving the CCD corresponding to each pixel is given by

$$V = g(KI + N_{\text{Shot}} + N_{\text{PRNU}} + N_{\text{Floor}}) + N_I + N_Q, \quad (6)$$

where K is a constant parameter characterizing the photoelectric conversion efficiency.

From Eq. (6), we know that the valid video signal is irradiance intensity and analog gain dependent. For the given irradiance intensity, the expected value of the valid signal is

$$u(V_{\text{valid}}) = g(KI). \quad (7)$$

Therefore, the enlarged valid video signal will increase linearly with the gain factor.

Given a fixed CCD sampling frequency, all noise sources are considered additive Gaussian distributed, so the variance of Eq. (6) is given by

$$\delta_v^2 = g^2 K^2 \delta^2(I) + g^2(\delta_{\text{Shot}}^2 + \delta_{\text{PRNU}}^2 + \delta_{\text{Floor}}^2) + \delta_I^2 + \delta_Q^2$$
$$= g^2 \langle N_{\text{Shot}}^2 \rangle + g^2 \langle N_{\text{PRNU}}^2 \rangle + g^2 \langle N_{\text{Floor}}^2 \rangle$$
$$+ \langle N_I^2 \rangle + \langle N_Q^2 \rangle. \quad (8)$$

It could be seen that the variance of the photon shot noise, the PRNU noise, and the floor noise increase linearly with analog gain factor.

The analog gain is multiplied by the analog signal to increase the signal strength. Thus the valid signal power is given by

$$S = g^2 I_s = g^2 \frac{e^2 \eta^2 \lambda^2 P_S^2 R}{4 h^2 c^2}, \quad (9)$$

where I_s represents the valid signal power when analog gain factor equals 1, and the other definitions of the mentioned variables are summarized in Table. 1.

The SNR metrics proposed in [10–12] compare signal power to the noise power; then the CCD SNR formulation is expressed as

$$\text{SNR} = \frac{g^2 I_S}{g^2 \langle N_{\text{Shot}}^2(P_S + P_B) \rangle + g^2 \langle N_{\text{PSNU}}^2(P_S + P_B) \rangle + g^2 \langle N_{\text{Floor}}^2 \rangle + \langle N_I^2 \rangle + \langle N_Q^2 \rangle}. \quad (10)$$

Replacing the CCD noise variance with the quadratic equation given in Eq. (5), we obtain

$$\text{SNR}(I, g) = \frac{I_s}{AI^2 + BI + C + Dg^{-2}}. \quad (11)$$

From Eq. (11) we could see obviously that the proportion of the quantization noise to the CCD total

Table 1. CCD Noise Sources and Their Formulas[a]

Noise type	Noise equivalent power
N_{shot}, photon shot noise	$\langle N_{\text{shot}}^2(P_S + P_B) \rangle = \frac{\eta \lambda e^2 B R}{2hc}(P_S + P_B)$
N_{PRNU}, photo response nonuniformity noise	$\langle N_{\text{PRNU}}^2(P_S + P_B) \rangle = \frac{U_1 \eta^2 \lambda^2 e^4 B^2 R^2}{4h^2 c^2}(P_S + P_B)^2$
N_{Dark}, dark current shot noise	$\langle N_{\text{Dark}}^2 \rangle = \frac{e J_D A_D B R}{2}$
N_{FPN}, fixed pattern noise	$\langle N_{\text{FPN}}^2 \rangle = \frac{U_2 J_D^2 A_D^2 B^2 R^2}{4}$
N_T, thermal noise	$\langle N_T^2 \rangle = 4KT_{\text{Previous}}B$
N_I, amplifier intrinsic noise	$\langle N_I^2 \rangle = 4KT_{\text{Post}}B$
N_Q, quantization noise	$\langle N_Q^2 \rangle = \frac{q^2}{12}$

[a]where P_S represents the signal incident power upon the detector, and P_B represents the background incident power upon the detector, η represents the quantum efficiency, λ represents the wavelength, e represents the charge of an electron, B represents noise equivalent bandwidth, R represents the load resistor, h represents Planck's constant, c represents the speed of light, J_D represents the dark current density, A_D represents the pixel area, U_1 represents the photon response nonuniformity ratio, U_2 represents the fixed pattern noise ratio, K represents the Boltzmann constant, T_{Previous} represents the temperature of the previous circuit of the amplifier, and T_{Post} represents the temperature of the post circuit of the amplifier.

noise will fall with the analog gain; then the CCD SNR will increase accordingly, and its augmenter with the analog gain is given by

$$\Delta\text{SNR}_{g_1 g_2}(I) = \frac{I_s}{AI^2 + BI + C + Dg_2^{-2}}$$
$$- \frac{I_s}{AI^2 + BI + C + Dg_1^{-2}}, \qquad (12)$$

where g_1 represents the original gain factor, and g_2 represents the amplified gain factor. Usually the SNR is expressed in decibels, so that Eq. (12) becomes

$$\Delta\text{SNR}_{g_1 g_2}(I)$$
$$= 10 \log \left(1 + \frac{g_1^{-2} - g_2^{-2}}{A \cdot D^{-1}I^2 + B \cdot D^{-1}I + C \cdot D^{-1} + g_2^{-2}} \right) \text{dB},$$
$$(13)$$

assuming that g_3 represents another amplified gain factor, and $g_3 - g_2 = g_2 - g_1$. As deduced in Appendix A, we obtain

$$\Delta\text{SNR}_{g_1 g_2}(I) > \Delta\text{SNR}_{g_2 g_3}(I), \qquad (14)$$

which indicates that the analog gain amplification in the initial stage does more contributions to the total CCD SNR improvement, while as the gain factor keeps increasing, the benefits to the CCD SNR will decrease gradually, then eventually to zero. In that case the CCD SNR will approach its theoretical maximum value

$$\max(\text{SNR}(I)) = \frac{I_s}{AI^2 + BI + C}. \qquad (15)$$

B. Mathematical Models of the Dynamic range with the Analog Gain

The dynamic range is defined as the maximum signal divided by the noise floor. The SNR approximates the dynamic range only when the system is noise-floor limited. In practice, the actual SNR would never reach the value suggested by the dynamic range. In the CCD-based imaging systems, the dynamic range is used to select the appropriate A/D converter. This assures that a low-contrast target could be detected.

There are two types of definitions about the CCD dynamic range; the first one relates to electrics, and the second one relates to optics.

The electrics dynamic range could be expressed as

$$\text{DR}_E(g) = \frac{S_{\text{sat}}}{N_{\text{noise}}} = \frac{S_{\text{sat}} / N_{\text{floor}}}{g + (N_Q + N_I) / N_{\text{floor}}}, \qquad (16)$$

where S_{sat} is the CCD average maximum output level for a specified light input, the S_{sat} is typically

248 digital number (DN) for 8 bits A/D converter or 3950 DN for 12 bits A/D converter, and N_{noise} is the standard deviation of the CCD outputs when measured in the dark environment. Equation (16) indicates that the electric dynamic range is a function of amplifier gain, signal magnitude, and electrical frequency, due to the fact that the floor noise (which is a combination of the dark current noise, the fixed pattern noise, and the thermal noise), the amplifier intrinsic noise, and the A/D converter quantization noise are all noise equivalent bandwidth independent.

The decreasing gradient of Eq. (16) is given by

$$\frac{\partial(\text{DR}_E(g))}{\partial g} = -\frac{S_{\text{sat}} / N_{\text{floor}}}{(g + (N_Q + N_I) / N_{\text{floor}})^2}. \qquad (17)$$

Generally, the magnitudes of the quantization noise and the amplifier intrinsic noise are far less than the correspondence of the floor noise, so Eq. (17) could be approximately written as

$$\frac{\partial(\text{DR}_E(g))}{\partial g} \approx -\frac{S_{\text{sat}} / N_{\text{floor}}}{g^2}. \qquad (18)$$

However, in some special applications, the quantization noise may dominate the CCD floor noise. In such a case, the shape of the decreasing gradient curve is relatively flat compared to the correspondence given in Eq. (18).

The optics dynamic range could be defined as

$$\text{DR}_O = \frac{S_{\text{EE}}}{N_{\text{EE}}}, \qquad (19)$$

where S_{EE} represents the signal equivalent exposure level that produces a saturation output S_{sat}, and N_{EE} represents the noise equivalent exposure level that produces the output N_{noise}. As mentioned above, the N_{EE} could also be divided into three parts, the floor noise equivalent exposure level N_{FEE}, the amplifier intrinsic noise equivalent exposure level N_{IEE}, and the quantization noise equivalent exposure level N_{QEE}. Similar to the electric dynamic-range definition, we obtain

$$\text{DR}_O(g) = \frac{S_{\text{EE}}}{gN_{\text{FEE}} + N_{\text{IEE}} + N_{\text{QEE}}}. \qquad (20)$$

Assuming that the ratio of the equivalent exposure level to the CCD corresponding output level is equal to k, then Eq. (20) could be written as

$$\text{DR}_O(g) = \frac{kS_{\text{sat}}}{kg \cdot N_{\text{floor}} + kN_I + kN_Q} = \text{DR}_E(g), \quad (21)$$

which indicates that the optics and electrics dynamic range could be normalized to the same formulas. The conclusion drawn above is also applicable to the

optics dynamic range except the signal and noise magnitudes. For the electrics dynamic range, as stated above, the maximum signal only depends on the CCD camera output resolution, while the noise magnitude with the analog gain is given by

$$N_{\text{noise}} = g \cdot N_{\text{floor}} + N_I + N_Q. \qquad (22)$$

However, we know that when analog gain increases by the g times, the amount of the equivalent exposure will decrease by the same factor when producing the equal intensity of the CCD outputs, so both the saturation and noise equivalent exposure level will decrease with the analog gain; then the scope of the CCD equivalent exposure with the analog gain is given by

$$\left(N_{\text{FEE}} + \frac{N_{\text{IEE}} + N_{\text{QEE}}}{g}, \frac{S_{\text{EE}}}{g} \right). \qquad (23)$$

Optics dynamic range is more favorable for camera designers, since it not only demonstrates the ratio of the maximum signal to the minimum signal, but also reveals the CCD minimum detectable irradiance and the maximum acceptable irradiance.

C. Design Trade-off Between the CCD SNR and Dynamic Range with the Analog Gain

SNR and dynamic range are the two key parameters characterizing the CCD performance. However, the latter plays a more important role than the former, which indicates that a picture with a relatively lower SNR value is always better than the one full of saturation pixels. The balance of the CCD SNR and dynamic range will be analyzed mainly based on two situations: (1) the impact of quantization effect is neglected, which is tenable in most general imaging and machine vision applications, (2) the quantization noise dominates the floor noise, which may occur in remote sensing systems, especially for military applications.

For the first situation, the amount of the CCD SNR increment caused by analog gain adjustment is given by Eq. (12). In most cases, the value is inappreciable. However, according to Eq. (17), the dynamic range degradation is relatively huge, so it is unnecessary to change the gain factor.

For the second situation, there exist two restrictions when searching for the appropriate analog gain factor. First, assuming that the equivalent exposure intensity generated by the interested target is within $(T_{\text{LE}}, T_{\text{HE}})$, then the range of the CCD equivalent exposure intensity is limited by Eq. (23). Taking advantage of the CCD dynamic range, the scope of the detector irradiance responsivity should match with the scope of the interested target irradiance intensity as much as possible. So it is required that $N_{\text{FEE}} + \frac{N_{\text{IEE}} + N_{\text{QEE}}}{g} \leq T_{\text{LE}} < T_{\text{HE}} \leq \frac{S_{\text{EE}}}{g}$, and the gain factor should be within $g \leq \max(1, \tilde{S}_{\text{EE}}/T_{\text{HE}})$.

Second, as suggested above, the decreasing gradient of Eq. (17) is relatively flat when compared to the correspondence of the first situation. Therefore, as long as the analog gain factor is less than the given value, such as $g < g'$, the dynamic range degradation is acceptable.

For optimizing the CCD performance, it is necessary that the above two requirements should be satisfied simultaneously. In addition, as suggested in Eq. (13), the larger the analog gain factor becomes, the more SNR augmenter will be obtained. Therefore the optimal gain factor is equal to $\min(\max(1, S_{\text{EE}}/T_{\text{HE}}), g')$.

4. Experiment of Radiometric Calibration

The diagram of the calibration platform is shown in Fig. 2, and the practical experimental devices are illustrated in Fig. 3. An integrating sphere is used to provide the even illumination. A customized CCD without imaging lens and its driving circuits are mounted on a guide rail, which is separated from the ground by the optics vibration isolation platform. The captured images are transmitted to the work station through Camera Link Interface, and the camera configuration parameters are adjusted by external acquisition software through the interface. The experiment is performed at an ambient temperature around 22 °C, where the CCD temperature is approximately 35 °C.

During the experimental procedure, we adopt two types of feedback mechanisms to improve the calibration accuracy. First, in order to have a stable and continuous light source, a calibrated illuminometer is used to make a relative calibration of the beam exiting from the integrating sphere. As long as the illumination uniformity of the light beam exceeds the given threshold, the integrating sphere control unit will adjust the corresponding parameters, which ensure that the integrating sphere could provide a highly uniform illumination. Second, due to the fact that the temperature has a significant influence on the CCD noise measurement accuracies, a two-way
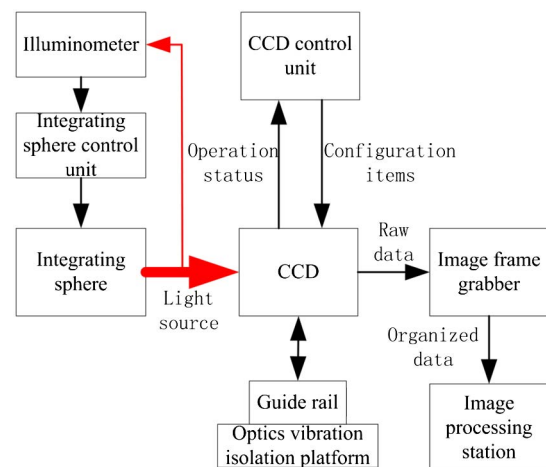

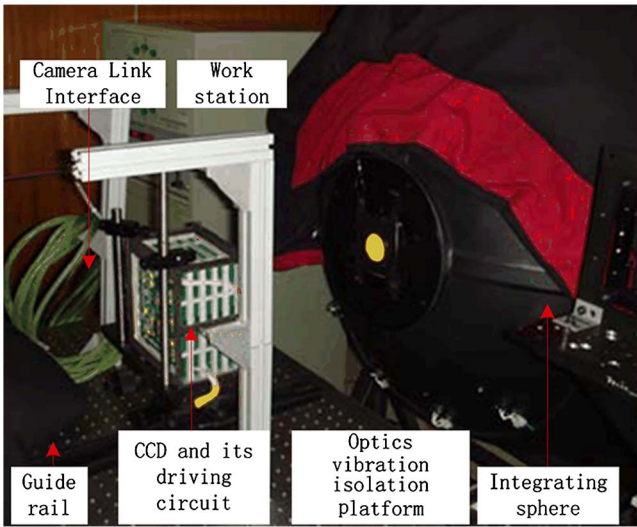Fig. 2. (Color online) Diagram of CCD calibration platform.

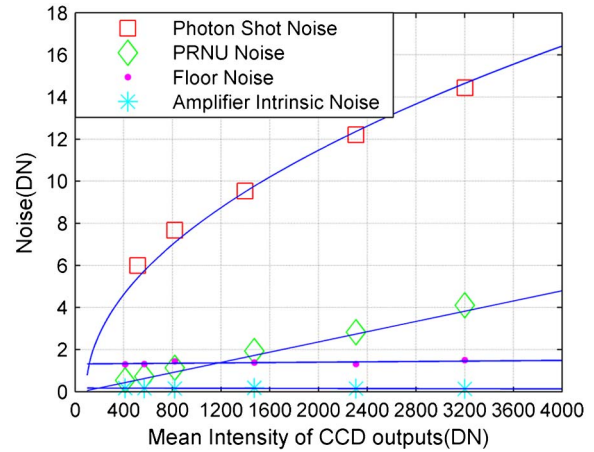Fig. 3. (Color online) Practical CCD calibration platform.

Fig. 4. (Color online) CCD noises as a function of pixel mean intensity. Data points correspond to individual measurements at different illuminations by adjusting the integrating sphere luminance, while the solid lines represent the predicted curves.

communication scheme between the tested CCD and its control unit is adopted. In this way, each calibration image will own its unique mark that records the experimental temperature, line frequency, and exposure time. In the noise-processing procedure, the frames that have the same testing conditions are classified as the candidate samples.

The features of the tested CCD are summarized in detail in Table 2.

A. Measuring CCD Noises

The CCD noise measurement methods have already been well studied [12–16]. In this paper, we adopt the means proposed in [16] to develop the tested CCD noise models. The test condition is described as follows: the CCD analog gain factor is set to 1, and the quantization step is set to 12 bits; then we draw the relative magnitudes of the first three noise components in Fig. 4.

From Eq. (3), we know that the PRNU noise increases almost linearly with the incident signal, so the best-fit expression for the PRNU noise is given by

$$N_{\mathrm{PRNU}} = 0.00121552\bar{u}, \tag{24}$$

where $\bar{u}$ represents mean DN of the CCD outputs.

A slight trend can be seen that the photon shot noise has $N_S \approx \sqrt{\bar{u}}$ as expected from the Poisson sampling theorem for sampling of discrete quanta; therefore, a square-root curve is fitted for the measured N_S

$$N_{\mathrm{shot}} = 0.0692\sqrt{\bar{u}}. \tag{25}$$

The floor noise is the natural component existing in the CCD. It depends on the integration time as well as the ambient temperature, but it has nothing to do with the incident flux; hence the most suitable expression describing the measured floor noise is given by

$$N_{\mathrm{floor}} = 1.53. \tag{26}$$

As Table. 1 shows, the amplifier intrinsic noise depends on the temperature of the post amplifier circuit, and it also has no relationship with the incident flux. Since the testing temperature is relatively stable, the amplifier intrinsic noise is

$$N_I = 0.17. \tag{27}$$

From Fig. 4 we could find that for very low photon fluxes, the floor noise plays the main role. As the incident flux increases, the photon shot noise dominates. Finally, for very high flux level, the noise may be dominated by the PRNU noise. Moreover, we also find that the experimental results accord well with the theoretical models presented in Section 2, so these noise models will be used in the following studies.

Table 2. Detail Features of the Tested CCD (Provided by the Manufacturer)

Parameter	Value
Native resolution	4008×5344
Pixel size (μm)	8
Full well capacity (e^{-1})	50,000
Quantum efficiency	40%
Sensitivity (DN /nJ /cm^2) @12 bit	10,000
Dynamic range	2500
Total floor noise (DN)	1.54
Saturation equivalent exposure (nJ /cm^2)	0.384
Noise equivalent exposure (pJ /cm^2)	0.192
Camera output resolution (bit)	8, 10, 12
Line rate (kHz)	20
Initial analog gain	1
Initial digital gain	1

B. Effect of Analog Gain on the CCD Individual Noise Sources

In Subsection 3.A, we propose that the valid video signal, the photon shot noise, the PRNU noise, and
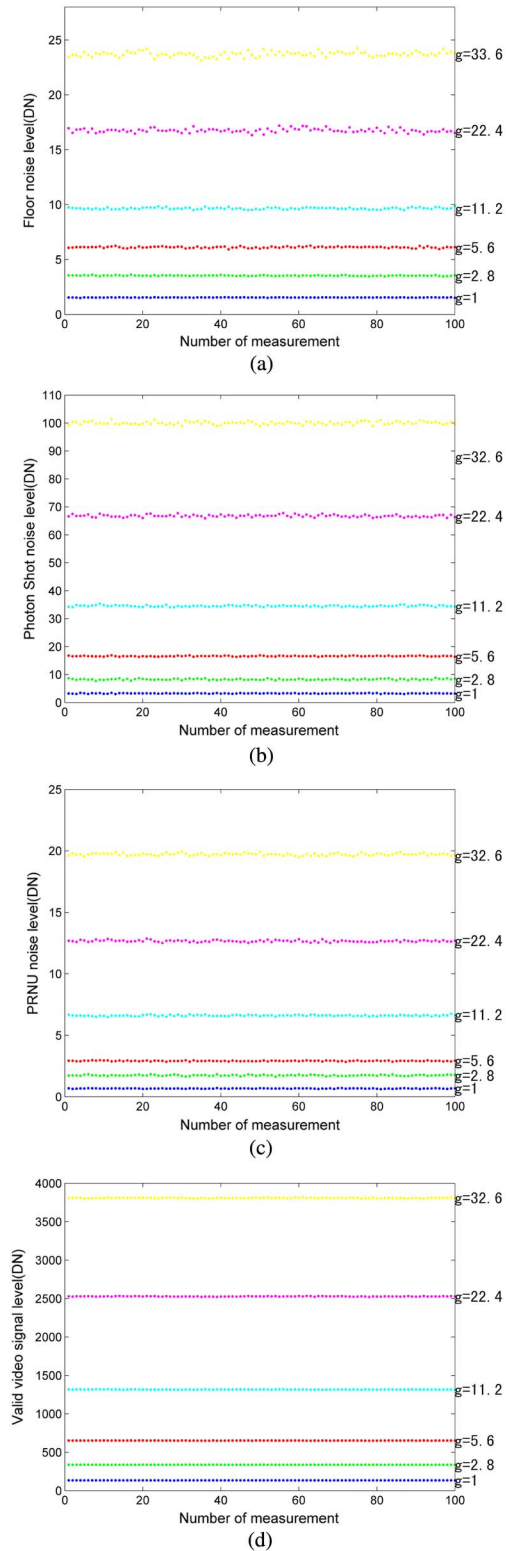
Analog gain	Signal (DN)	N_{shot} (DN)	N_{PRNU} (DN)	N_{floor} (DN)
1	134	3.28	0.72	1.54
2.8	337	8.30	1.87	3.65
5.6	651	16.84	3.24	5.93
11.2	1317	34.55	6.96	9.74
22.4	2527	66.92	13.45	16.58
32.6	3809	100.09	20.68	23.63

the floor noise will increase linearly with the analog gain. Since the assumption is the key point for investigating the relationship among the CCD SNR, the dynamic range, and the analog gain, it is required to test it experimentally.

In our experiment, the A/D converter resolution is set to 12 bits to eliminate the quantization effect

Fig. 5. (Color online) Experimental results of the floor noise, the photon shot noise, the PRNU noise, and the valid video signal in the 100 independent measurements.
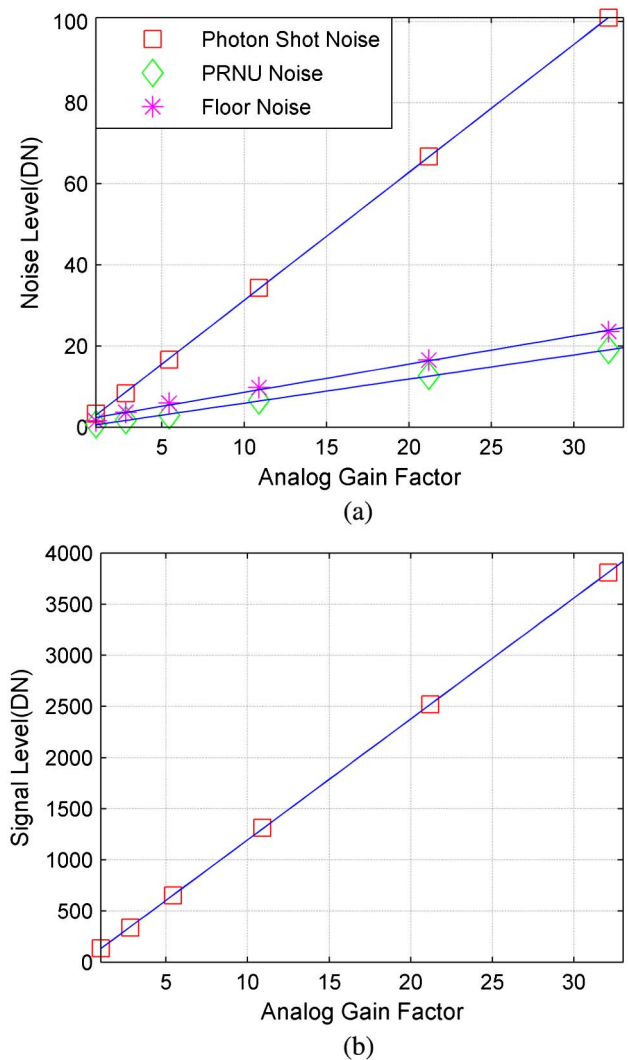

Fig. 6. (Color online) (a) CCD noises and (b) video signal as a function of the analog gain factor. Data points correspond to expected measurement values at the analog gain factors of 1, 2.8, 5.6, 11.2, 22.4, and 33.6, respectively, while the solid lines represent the fitting lines.

when measuring the CCD noise. Both the noises and the valid signal are measured by making 100 independent measurements at each analog gain factor. The floor noise is measured with no light incident onto the CCD for eliminating photoelectron effect.

For evaluating the photon shot noise, the PRNU noise, and the valid video signal, the integrating sphere luminance is set to 2.86 cd /m^2, and the integration time is set to 0.5 ms, which ensures that the analog gain could be adjusted in a wide range
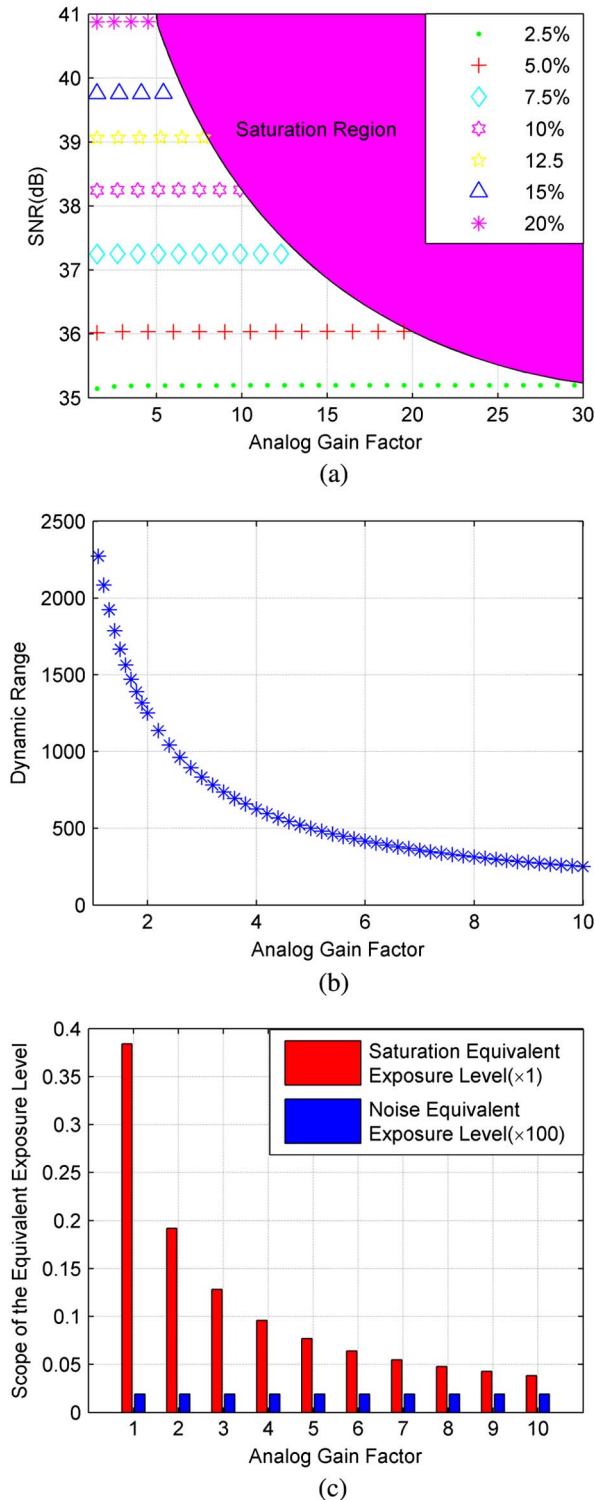

Fig. 7. (Color online) (a) CCD SNR at the 2.5% to 20% of the saturation exposure level, (b) CCD dynamic range, and (c) scope of the CCD equivalent exposure level as a function of the analog gain factor according to the first situation.
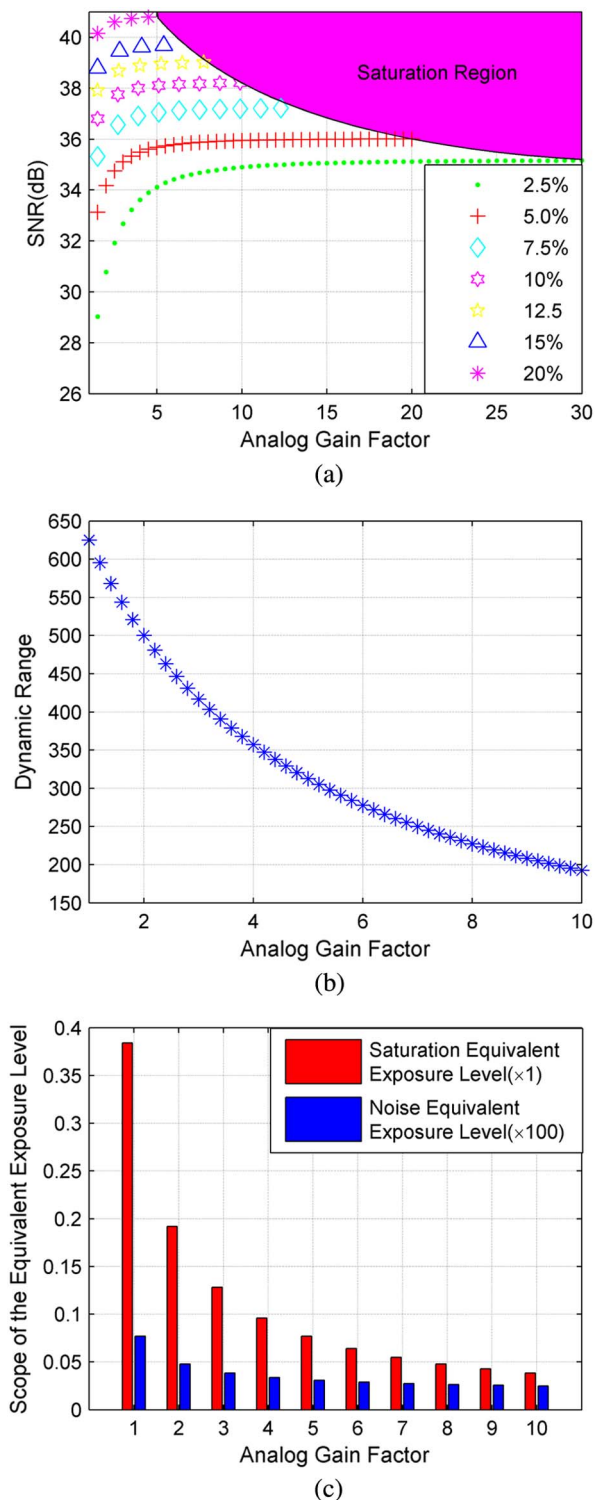

Fig. 8. (Color online) (a) CCD SNR at the 2.5% to 20% of the saturation exposure level, (b) CCD dynamic range, and (c) scope of the CCD equivalent exposure level as a function of the analog gain factor according to the second situation.

Table 4. Optics and Environmental Conditions of the Imaging System

Parameter	Value
Optics aperture diameter (mm)	242
Focal length (mm)	1800
Spectral band pass (μm)	0.4 to 0.9
Optics transmission	0.7
Imaging distance (km)	1
Look angle (deg)	30
Sun angle (deg)	35
Atmosphere	Middle latitude, summer, 15 km visibility

without setting the video signal to saturation. The obtained experimental results are illustrated in Figs. 5(a)–5(d).

The expected values of the 100 independent measurements are summarized in Table. 3.

In order to investigate the relationship between the noise and the signal with the analog gain, the fitting equations on the obtained expected measurement values with the analog gain are given by

$$N_{\text{Floor}} = 0.6595g + 1.7587,$$
$$N_{\text{PRNU}} = 0.6099g + 0.0342,$$
$$N_{\text{Shot}} = 2.9737g + 0.3663,$$
$$I_s = 112.45g + 26.881. \tag{28}$$

Figures 6(a) and 6(b) show the expected value of the floor noise, the photon shot noise, the PRNU noise, and the valid video signal with the analog gain in the 100 independent measurements, and the best

fitting lines determined by Eq. (28) are also plotted. It could be seen that the floor noise, the photon shot noise, the PRNU noise, and the valid video signal increase approximately linearly with the analog gain. The experimental results tell us that the conclusion proposed in Subsection 3.A is reasonable.

C. Effect of Analog Gain on the CCD SNR and Dynamic Range

The effects of the analog gain on the CCD SNR and the dynamic range will be evaluated based on the two situations that have been discussed in Subsection 3.C.

When the camera output resolution is set to 12 bits, the quantization noise equals 0.29 DN, which is far less than the measured floor noise given in Eq. (26), so the requirement of situation one is satisfied. We use seven different exposure levels to evaluate the relationship between the CCD SNR and the analog gain. Substituting the noises developed in Eqs. (24)–(27) into the SNR formula given in Eq. (10), we plot the CCD SNR versus the gain factors in Fig. 7(a). We could obviously find that the shapes of the CCD SNR curves are effectively flat showing no apparent trend of increase with the analog gain. However, according to Eqs. (17) and (23), the CCD dynamic range as well as the scope of the CCD equivalent exposure level decrease linearly with the analog gain, which is shown in Figs. 7(b) and 7(c). Therefore it is unnecessary to change the CCD SNR in the first situation.

When the camera output resolution is set to 8 bits, the added quantization noise is equal to 4.64 DN, which dominates the CCD floor noise given in Eq. (22); therefore, the requirements of situation
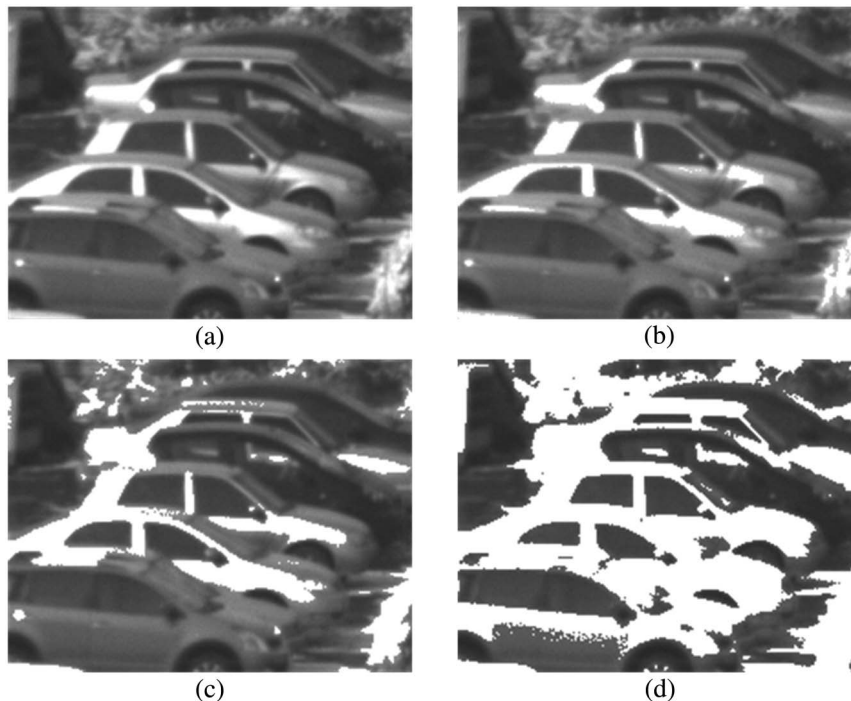

Fig. 9.   Images obtained with analog gain factor of (a) 1, (b) 2, (c) 3, and (d) 4 based on the first situation, and the corresponding digital gain is 1, 1/2, 1/3, and 1/4.
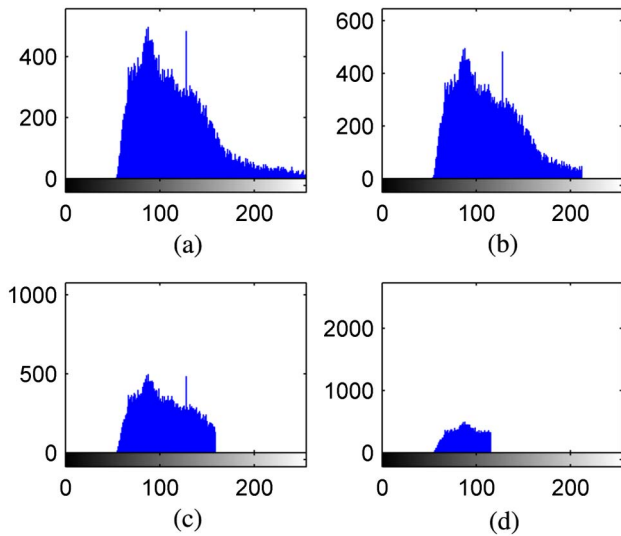
Fig. 10. (Color online) Histogram of the images obtained with analog gain factor of (a) 1, (b) 2, (c) 3, and (d) 4 based on the first situation.

two are satisfied. Without loss of generality, we also use the same seven exposure levels for investigation. The SNR values at the individual gain factor are illustrated in Fig. 8(a). It shows that the magnitudes of the SNR increase with the analog gain, especially at the initial gain amplification stage, which does the greatest contributions to the total SNR augmenter. However, as the gain factor continues to increase, the further attainable SNR augmenter is quite limited. Then, according to Eq. (16), we plot the dynamic range versus the analog gain in Fig. 8(b). Compared

to the curve shown in Fig. 7(b), the curve illustrated in Fig. 8(b) decreases gently. Noting that the irradiance of the interested target varies with the sun angle, target reflectivity, etc., it is required that the scope of the CCD equivalent exposure shown in Fig. 8(c) should be as wide as possible. Therefore, the analog gain factor is generally set to two to four times in practical applications. In this way, it will not only improve the CCD SNR greatly, but also hold the dynamic range wide enough.

5. Experiment of Imaging in Practice

SNR is a common metric used to tell the image quality and radiometric performance of a remote sensing system. However, when a camera designer specifies a SNR value, it is not always sure how it relates to the image quality of the system [17,18]. To accurately compare the performance of the system with different analog gain, a standard set of images would need to be defined and acquired. We have established an imaging platform, from which the images with different signal levels could be obtained. The descriptions of the camera detector are listed in Table 2, and the optics parameters as well as the imaging conditions are summarized in Table 4.

Similar to the analysis presented in Subsections 3.C and 4.C, the effect of the analog gain on the image quality will also be evaluated in two cases, where (1) the impact of quantization effect is neglected, and (2) the quantization noise dominates the floor noise [19].

Figure 9 shows a subsection of the obtained images with the analog gain of 1, 2, 3, and 4 for the first case,
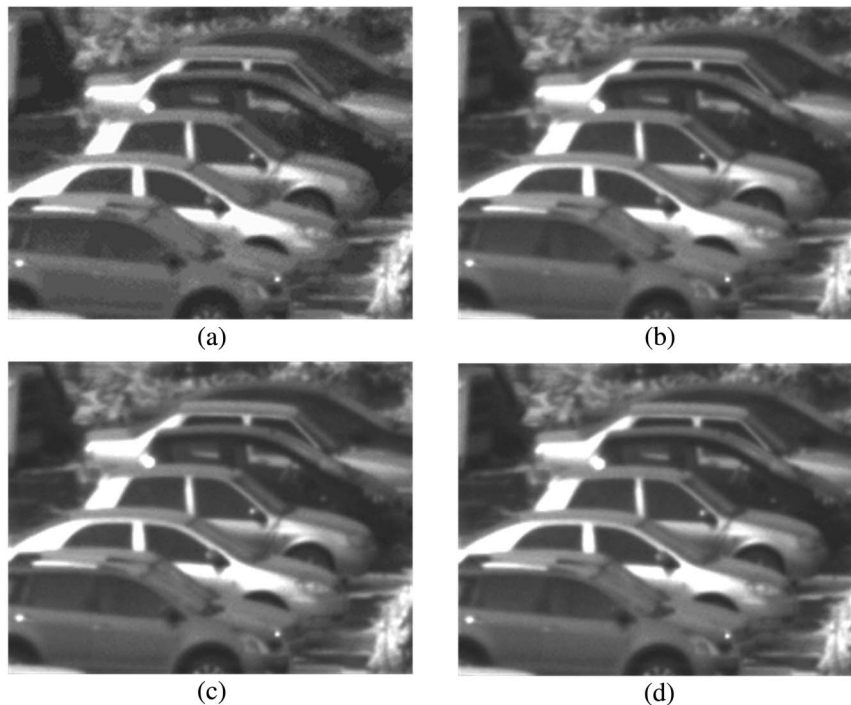

Fig. 11. Images obtained with analog gain factor of (a) 1, (b) 2, (c) 4, and (d) 8 based on the second situation, and the corresponding digital gain is 4, 4/2, 4/3, and 4/1.

where the CCD output resolution is 12 bits, and Fig. 10 illustrates the corresponding histograms. As we know, the digital gain adjustment is a pure mathematical operation to the captured images; the signals including the valid video and the corresponding noises are increased by the same factor, so it is irrelevant to the CCD SNR, and thus it will not affect the CCD SNR evaluation results. Therefore, in order to ensure the pixel mean intensities of Figs. 9(a)–9(d) are equal to each other, it is required that the product of the analog and digital gain factor are the same.

An image whose pixels tend to occupy the entire range of possible gray levels and, in addition, tend to be distributed uniformly, will have an appearance of high contrast and will exhibit a large variety of gray tones. From Figs. 9(a) and 10(a), we see that the components of the histogram in the high-contrast image cover a broad range of the gray scale and, further, that the distribution of pixels is not too far from uniform, with very few vertical lines being much higher than the others. From Fig. 9(b) we find that the image quality improvement with the analog gain increment is quite limited when compared to the original scene illustrated in Fig. 9(a). Simultaneously, the histogram shown Fig. 10(b) is narrow and is centered toward the middle of the gray level. As the analog gain keeps increasing, too many saturation pixels are added to Figs. 9(c) and 9(d) and the images are dominated by large saturation areas, resulting in a histogram characterized by a large concentration of pixels in the light end of the gray scale, which could be seen in Figs. 10(c) and 10(d). Finally, it is reasonable to conclude that the image interpretability is degraded, and the dynamic range is decreased with the gain factor increasing.

Figure 11 shows a subsection of the obtained images with the analog gain of 1, 2, 4, and 8 for the second case, where the CCD output resolution is
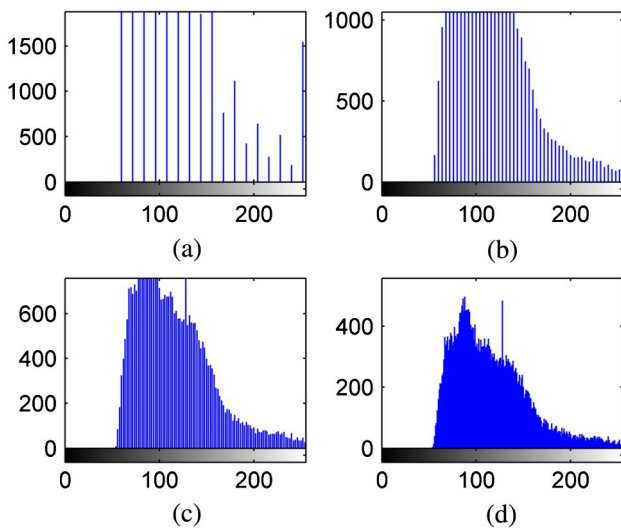
8 bits. It could be seen apparently that Fig. 11(a) exhibits too much mosaic effect, and the corresponding histogram shown in Fig. 12(a) distributes discretely, which indicates that the detail information of the target is lost. Meanwhile, Figs. 11(b)–11(d) show more scene details, especially near the edge of the cars. Moreover, it is almost impossible to distinguish the differences among Figs. 11(b)–11(d) with unaided eyes. From the histograms illustrated in Figs. 12(b)–12(d), we could see that the histogram becomes dense with the analog gain increment, which means that the image interpretability is improved. The experiment indicates that the initial analog gain amplification has the most contributions to the image quality, and as the gain factor continues to increase, the image quality improvement becomes inconspicuous.

6. Conclusion

The effects of the analog gain to the CCD SNR and the dynamic range have been presented in this paper. The corresponding issues are investigated through both theoretical analyses and experiments, including radiometric calibration and imaging in practice. The conclusion is drawn based on two situations, (1) the influence of the quantization effect could be neglected, and (2) the quantization noise dominates the floor noise. For the first situation, the experimental results show that as the gain factor increases, the CCD SNR augmenter is less than 0.1 dB until the CCD approaches saturation status, and the image quality improvement is almost inconspicuous. However, the CCD dynamic range decreases with the analog gain dramatically, which results in the scene detail losses. Therefore, there is no need to adjust the gain factor in such a situation. For the latter situation, the CCD SNR increases with the analog gain, especially during the initial gain amplification stage. Moreover, the decreasing slope of the dynamic range curve is relatively flat. Hence, the analog gain factor is usually increased by two to four times in practical applications. In this way, the CCD SNR and the image quality will be improved as well as possible, while the dynamic range can be held wider enough. We hope that the mathematical models and experimental results presented here would be useful for the camera designers, especially for remote sensing applications.

Fig. 12. (Color online) Histogram of the images obtained with analog gain factor of (a) 1, (b) 2, (c) 4, and (d) 8 based on the second situation.

Appendix A

$$\Delta SNR_{g_1 g_2}(I) - \Delta SNR_{g_2 g_3}(I)$$
$$= 10 \log \left(1 + \frac{g_1^{-2} - g_2^{-2}}{A \cdot D^{-1} I^2 + B \cdot D^{-1} I + C \cdot D^{-1} + g_2^{-2}} \right)$$
$$- 10 \log \left(1 + \frac{g_2^{-2} - g_3^{-2}}{A \cdot D^{-1} I^2 + B \cdot D^{-1} I + C \cdot D^{-1} + g_3^{-2}} \right),$$
$$(A1)$$

where $g_3 > g_2 > g_1 > 1$, and $g_3 - g_2 = g_2 - g_1$.

For deducing simplicity, let that

$$A \cdot D^{-1} I^2 + B \cdot D^{-1} I + C \cdot D^{-1} = k_1 \cdot g_2^{-2} = k_2 \cdot g_3^{-2}, \tag{A2}$$

where k_1 and k_2 represent the coefficients of proportionality. Substituting Eq. (A2) into Eq. (A1), we obtain

$$\Delta \mathrm{SNR}_{g_1 g_2}(I) - \Delta \mathrm{SNR}_{g_2 g_3}(I)$$
$$= 10 \log \left(1 + \frac{g_1^{-2} \cdot g_2^2 - 1}{k_1 + 1} \right) - 10 \log \left(1 + \frac{g_2^{-2} \cdot g_3^2 - 1}{k_2 + 1} \right). \tag{A3}$$

As we know, the logarithmic function is a monotone increasing function; therefore comparison of $\Delta \mathrm{SNR}_{g_1 g_2}(I)$ and $\Delta \mathrm{SNR}_{g_2 g_3}(I)$ is equivalent to

$$\Delta \mathrm{SNR}_{g_1 g_2}(I) - \Delta \mathrm{SNR}_{g_2 g_3}(I) \quad \frac{g_1^{-2} \cdot g_2^2 - 1}{k_1 + 1} - \frac{g_2^{-2} \cdot g_3^2 - 1}{k_2 + 1}. \tag{A4}$$

Since $g_3 > g_2 > 1$, so that $k_1 < k_2$, we obtain

$$\frac{g_1^{-2} \cdot g_2^2 - 1}{k_1 + 1} - \frac{g_2^{-2} \cdot g_3^2 - 1}{k_2 + 1} > \frac{g_1^{-2} \cdot g_2^2 - 1}{k_1 + 1} - \frac{g_2^{-2} \cdot g_3^2 - 1}{k_1 + 1}$$
$$= \frac{1}{k_1 + 1} \left(\frac{g_2^2}{g_1^2} - \frac{g_3^2}{g_2^2} \right)$$
$$= \frac{1}{k_1 + 1} \frac{(g_2^2 - g_1 g_3)(g_2^2 + g_1 g_3)}{g_1^2 g_2^2}. \tag{A5}$$

Substituting $g_3 - g_2 = g_2 - g_1$ into the right side of Eq. (A5), we obtain

$$\frac{1}{k_1 + 1} \frac{(g_2^2 - g_1 g_3)(g_2^2 + g_1 g_3)}{g_1^2 g_2^2}$$
$$= \frac{1}{4(k_1 + 1)} \frac{(g_1 + g_3)(g_2^2 + g_1 g_3)}{g_1^2 g_2^2} > 0. \tag{A6}$$

Therefore $\frac{g_1^{-2} \cdot g_2^2 - 1}{k_1 + 1} - \frac{g_2^{-2} \cdot g_3^2 - 1}{k_2 + 1} > 0$; then from Eq. (A4) we know that $\Delta \mathrm{SNR}_{g_1 g_2}(I) > \Delta \mathrm{SNR}_{g_2 g_3}(I)$.

References

1. J. R. Janesick, Scientific Charge-Coupled Devices (SPIE Press, 2001).
2. G. C. Holst, CMOS/CCD Sensor and Camera Systems (SPIE Press, 2007).
3. M. Iyenqar and D. Lange, "The Goodrich 3rd generation DB-110 system: operational on tactical and unmanned aircraft," Proc. SPIE **6209**, 620909 (2006).
4. R. D. Fiete and T. Tantalo, "Comparison of SNR image quality metrics for remote sensing systems," Opt. Eng. **40**, 574–585 (2001).
5. N. J. Miller, M. P. Dierking, and B. D. Duncan, "Optical sparse aperture imaging," Appl. Opt. **46**, 5933–5943 (2007).
6. S. L. Smith, J. Mooney, T. Tantalo, and R. D. Fiete, "Understanding image quality losses due to smear in high-resolution remote sensing imaging systems," Opt. Eng. **38**, 821–826 (1999).
7. D. J. Wang, T. Zhang, and H. P. Kuang, "Clocking smearing analysis and reduction for multi phase TDI CCD in remote sensing system," Opt. Express **19**, 4868–4880 (2011).
8. A. V. Oppenheim and R. W. Schafer, Discrete-Time Signal Processing (Prentice Hall, 2009).
9. F. Devaux, J. L. Blanchet, and E. Lantz, "Effective signal-to-noise ratio improvement by parametric image amplification," Opt. Lett. **32**, 175–177 (2007).
10. R. H. Kingston, Detection of Optical and Infrared Radiation (Springer-Verlag, 1978).
11. G. C. Holst, CCD Arrays, Cameras, and Displays (SPIE Press, 1998).
12. P. X. Silveira and R. Narayanswamy, "Signal-to-noise analysis of task-based imaging systems with defocus," Appl. Opt. **45**, 2924–2934 (2006).
13. L. F. Chen, X. S. Zhang, J. M. Lin, and D. G. Sha, "Signal-to-noise evaluation of a CCD camera," Opt. Laser Technol. **41**, 574–579 (2009).
14. G. E. Healey and R. Kondepudy, "Radiometric CCD camera calibration and noise estimation," IEEE Trans. Pattern Anal. **16**, 267–276 (1994).
15. G. Zonios, "Noise and stray light characterization of a compact CCD spectrophotometer used in biomedical applications," Appl. Opt. **49**, 163–169 (2010).
16. K. Irie, A. E. Mckinnon, K. Unsworth, and I. M. Woodhead, "A technique for evaluation of CCD video camera noise," IEEE Trans. Circuit Syst. Video Technol. **18**, 280–284 (2008).
17. D. J. Wang and T. Zhang, "Noise analysis and measurement of time delay and integration charge coupled device," Chin. Phys. B **20**, 1–6 (2011).
18. G. C. Holst, Electro-Optical Imaging System Performance (SPIE Press, 2008).
19. G. C. Holst, "Imaging system performance based upon $F\lambda/d$," Opt. Eng. **46**, 103204 (2007).